Journal of Solid State Chemistry 181 (2008) 3051–3056

Contents lists available at ScienceDirect

Journal of Solid State Chemistry

journal homepage: www.elsevier.com/locate/jssc

Structural and magnetic characterisation of Aurivillius material $Bi_2Sr_2Nb_{2.5}Fe_{0.5}O_{12}$

E.E. McCabe [1], C. Greaves *

School of Chemistry, University of Birmingham, Edgbaston, Birmingham B15 2TT, UK

ARTICLE INFO

Article history:
Received 25 April 2008
Received in revised form
30 July 2008
Accepted 3 August 2008
Available online 14 August 2008

Keywords:
Aurivillius materials
Rietveld refinement

ABSTRACT

The $n = 3$ Aurivillius material $Bi_2Sr_2Nb_{2.5}Fe_{0.5}O_{12}$ is investigated and combined structural refinements using neutron powder diffraction (NPD) and X-ray powder diffraction data (XRPD) data reveal that the material adopts a disordered, tetragonal ($I4/mmm$) structure at temperatures down to 2 K. Significant ordering of Fe^{3+} and Nb^{5+} over the two B sites is observed and possible driving forces for this ordering are discussed. Some disorder of Sr^{2+} and Bi^{3+} over the M and A sites is found and is consistent with relieving strain due to size mismatch. Highly anisotropic thermal parameters for some oxygen sites suggest that the local structure may be slightly distorted with some rotation of the octahedra. Magnetic measurements show that the material behaves as a Curie–Weiss paramagnet in the temperature range studied with no evidence of any long-range magnetic interactions. Solid solutions including $Bi_{3-x}Sr_xNb_2FeO_{12}$, $Bi_2Sr_{2-x}La_xNb_2FeO_{12}$ and $Bi_2Sr_2Nb_{3-x}Fe_xO_{12}$ were investigated but single-phase materials were only successfully synthesised for a narrow composition range in the $Bi_2Sr_2Nb_{3-x}Fe_xO_{12}$ system.

1. Introduction

Aurivillius materials are a class of layered perovskite-related materials of general formula $M_2A_{n-1}BnO_{3n+3}$, composed of alternating fluorite-like $[M_2O_2]^{2+}$ and perovskite-like $[A_{n-1}B_nO_{3n+1}]^{2-}$ blocks. The M cation site is always at least partially occupied by Bi^{3+}, whereas the A cation site can be occupied by Bi^{3+}, or by a spherical cation such as a lanthanide or a group II metal. The B cations are smaller and are almost exclusively d^0 transition metals such as Ti^{4+}, Nb^{5+} or W^{6+} [1].

Aurivillius materials are well known for commonly exhibiting ferroelectric behaviour. They have been the focus of renewed interest in the light of recent reports of the fatigue-free behaviour of $SrBi_2Ta_2O_9$ in thin film form, which has resulted in their use as non-volatile ferroelectric random access memories [2]. It has been suggested by Yee et al. [3] that Aurivillius materials might display interesting electromagnetic properties if they could contain transition metals with partly filled d orbitals. In recent years, there has been increased interest in incorporating magnetic cations into the B sites in Aurivillius materials, not only with the goal of obtaining new magnetic materials structurally related to the magnetically interesting Ruddlesden–Popper phases, but also as a means of developing potential multiferroic materials in which both magnetic order and ferroelectric behaviour are coupled.

A well-characterised example of an Aurivillius material incorporating magnetic cations on the B site is $Bi_5Ti_3FeO_{15}$, which contains Fe^{3+} and Ti^{4+} statistically distributed over the B sites [4,5]. Manganese cations have also been incorporated into $n = 3$ Aurivillius materials [6,7]. Recently, a number of solid solutions of Aurivillius materials containing magnetic cations have been reported, from the magnetically dilute $Bi_2Sr_2Nb_2Ti_{1-x}M_xO_{12-\delta}$ (M = Fe, Cr, Mn, $x \leqslant 0.2$) [8] to several systems containing higher concentrations of magnetic cations: Tripathy et al. reported the series of polar Aurivillius phases $Bi_4Ti_{3-x}M_xFe_xO_{12}$ ($x = 0.25$ and 0.5 for M = Nb and $x = 0.25$ for M = Ta) and two centrosymmetric ruthenium phases $Bi_2Sr_2Nb_2RuO_{12}$ and $Bi_2Sr_2NaNb_2RuO_{12}$ [9] while Sharma et al. have also reported a number of new materials including $Bi_{1.5}Sr_{2.5}Nb_{2.5}Mn_{0.5}O_{12}$ and $Bi_{1.5}Sr_{2.5}Nb_{2.5}Ru_{0.5}O_{12}$ [10]. These last two materials are interesting for a number of reasons including the incorporation of magnetic M^{4+} cations into the Aurivillius B site, but also the high Sr:Bi ratio. The report by Mandal et al. of the synthesis and structural characterisation using X-ray powder diffraction data (XRPD) of the $n = 3$ Aurivillius phase $Bi_2Sr_2Nb_{2.5}Fe_{0.5}O_{12}$ [11] prompted us to investigate a number of $n = 3$ Aurivillius systems containing iron. We report here the synthesis of $Bi_2Sr_2Nb_{2.5}Fe_{0.5}O_{12}$ as well as its structural characterisation using neutron powder diffraction (NPD) data and its magnetic behaviour. The basic structure of

* Corresponding author.
E-mail address: c.greaves@bham.ac.uk (C. Greaves).
[1] Currently at Department of Engineering Materials, University of Sheffield, Sir Robert Hadfield Building, Mappin Street, Sheffield S1 3JD, UK

0022-4596/$ - see front matter © 2008 Elsevier Inc. All rights reserved.
doi:10.1016/j.jssc.2008.08.004

this material is given in a previous report [11] but we have been able to determine the degree of ordering of both niobium and iron over the *B* sites, and of bismuth and strontium over the *M* and *A* sites. The use of NPD in this study has also enabled the oxygen sites to be probed more sensitively. We discuss several structural features observed in the context of related materials recently reported.

2. Experimental

Polycrystalline samples of all materials were prepared by the solid-state reaction of stoichiometric quantities of high purity, Bi_2O_3, $SrCO_3$, La_2O_3, Nb_2O_5 and Fe_2O_3 (Aldrich, >99%). The reagents were intimately ground together and heated in air with intermittent grinding. Typical reaction conditions were 12 h at 820 °C, 12 h at 880 °C followed by 24 h at 920 °C and a final heating for 24 h at 1000 °C. A 7 g sample of $Bi_2Sr_2Nb_{2.5}Fe_{0.5}O_{12}$ was synthesised for structural and magnetic characterisation. Room temperature XRPD data were collected over a period of 10 h using a Siemens D5000 diffractometer (transmission mode, monochromated Cu$K\alpha_1$ radiation, step size 0.0199°, position sensitive detector). Time of flight (TOF) NPD data were collected at room temperature and 2 K at POLARIS (ISIS, UK). Rietveld structural refinements were carried out using the GSAS suite of programmes [12] Magnetic susceptibility measurements were carried out by *ac* excitation (amplitude 5 Oe) and *dc* extraction (field of 2000 Oe) using a quantum design physical properties measurement system. Diamagnetic corrections were applied.

3. Results and discussion

3.1. Investigation of possible solid solutions

The composition range $Bi_{3-x}Sr_xNb_2FeO_{12}$ ($0 \leqslant x \leqslant 0.8$) was investigated. For all compositions, an $n = 3$ Aurivillius phase was formed, but with significant amounts of $SrBi_2Nb_2O_9$ and the perovskite phase $Sr(Nb,Fe)O_3$. The perovskite content increased with *x* as the *B* cation oxidation state increased. It is thought that the $n = 3$ Aurivillius phase formed is bismuth and niobium rich. The composition range $Bi_2Sr_{2-x}La_xNb_2FeO_{12}$ ($0.2 \leqslant x \leqslant 1$) was also investigated and again, a small amount of $n = 3$ Aurivillius phase was formed, but with significant amounts of $SrBi_2Nb_2O_9$ and $Sr(Nb,Fe)O_3$. The $n = 3$ Aurivillius phase decomposed readily on heating.

The report by Mandal et al. [11] prompted us to investigate the composition range $Bi_2Sr_2Nb_{3-x}Fe_xO_{12}$ ($0.4 \leqslant x \leqslant 0.8$). Our results are in agreement with the report by Mandal et al. and suggest that there is only a narrow composition range that will form a stable product. For higher values of *x*, there were significant amounts of the perovskite impurity $Sr(Nb,Fe)O_3$, the perovskite content decreasing with *x*. However, both $Bi_2Sr_2Nb_{2.6}Fe_{0.4}O_{12}$ and $Bi_2Sr_2Nb_{2.5}Fe_{0.5}O_{12}$ could be synthesised. Initially, the samples contained an $n = 3$ Aurivillius phase, as well as some $SrBi_2Nb_2O_9$, but no perovskite content was visible from analysis of XRPD data. Further heating removed the $SrBi_2Nb_2O_9$ impurity to give single-phase products.

It was hoped that by investigating the limits to the solid solutions discussed above, an insight could be gained into the underlying crystal chemistry of these multilayer Aurivillius materials. The small size of the Fe^{4+} cation may limit the composition range in these materials. These observations are consistent with the recent literature on $n = 3$ Aurivillius phases in which only low concentrations of tetravalent cations with radii outside the limits suggested by Armstrong and Newnham [13] can be accommodated in the Aurivillius *B* site (for example $Bi_{1.5}Sr_{2.5}Nb_{2.5}Mn_{0.5}O_{12}$).

However, it is not immediately clear why the pure Fe^{3+} phases $Bi_3SrNb_2FeO_{12}$ and $Bi_2SrLaNb_2FeO_{12}$ were not successfully synthesised, when the $n = 4$ material $Bi_5Ti_3FeO_{15}$ can be formed [4,5]. The answer may lie in the size mismatch of the fluorite and perovskite blocks, which is greater for both $Bi_3SrNb_2FeO_{12}$ and $Bi_2SrLaNb_2FeO_{12}$ than for $Bi_5Ti_3FeO_{15}$ (although smaller than that of $Bi_2Sr_2Nb_{2.5}Fe_{0.5}O_{12}$, described below).

3.2. Structural refinement of $Bi_2Sr_2Nb_{2.5}Fe_{0.5}O_{12}$

A combined structural refinement was carried out using room temperature TOF NPD data from banks 1, 2 and 3 (E, C and A banks) and room temperature XRPD data. There was no evidence to suggest that the symmetry should be lowered and the refinement was carried out in space group *I*4/*mmm* using the atomic coordinates reported by Mandal et al. [11] as a starting model. The perovskite phase $Sr(Nb,Fe)O_3$ as well as Bi_2O_3 were included in the refinement as impurity phases but their content by weight was consistently ~0.2% and so we can be confident of the purity of the sample. The Rietveld refinement was carried out with background parameters (linear interpolation function), histogram scale factor, diffractometer zero points, lattice parameters, peak shape, atomic coordinates and anisotropic thermal parameters refined. Constraints were applied to the temperature factors of atoms on the same crystallographic site, and also to site occupancies to ensure that the stoichiometry remained constant and that each site was fully occupied. The fractional occupancies of the oxygen sites were refined but there was no significant deviation from full occupancy and these parameters were subsequently constrained at unity. As observed for related Aurivillius materials [14–17], refining the degree of ordering of bismuth and strontium over the *M* and *A* sites and niobium and iron over the *B* sites significantly improved the model and revealed some cation disorder.

However, the model obtained from this refinement had surprisingly anisotropic thermal parameters for the oxygen sites in the perovskite blocks, most notably for O(1), the equatorial oxygen in the central layer. The model suggested that the apical oxygens O(3) and O(4) showed increased motion in the *ab* plane; again, this is not unusual for this perovskite-related structure. However, the magnitude of the U_{22} parameter for O(1) ($0.184(2)$ Å^2) suggests a problem with the model. This U_{22} parameter reflects significant motion of the atom in the *b* direction, i.e., consistent with some rotation of the octahedra around the long axis. A disordered model was then used in the refinement with O(1) moved from the 4*c* site to the 8*i* site and the occupancy halved.

A combined structural refinement was also carried out using 2 K TOF NPD data from banks 1, 2 and 3 (E, C and A banks), in the same manner as described for the room temperature refinement. Again, unrealistic thermal parameters were obtained from the initial model with negative values for the central *B*1 site and highly anisotropic thermal parameters for the perovskite block oxygen sites, particularly O(1). As for the room temperature refinement, a disordered model was then used, with O(1) moved from the 4*c* site to the 8*i* site. This gave a more realistic model and an improvement in fit. There was no evidence of long-range magnetic order from the low-temperature NPD data.

It is noted that the models obtained from these refinements still show slightly anisotropic thermal parameters, particularly for the apical oxygen site O(4). However, moving this oxygen from the 4*e* site to the 16*m* site did slightly decrease the thermal parameters for this site but did not give any improvement in fit.

Aurivillius materials commonly undergo distortions to lower symmetry structures, these distortions comprising some rotation of the octahedra and sometimes displacement of cations in the structure. Odd-layer Aurivillius materials often undergo distortions which result in structures described by space group *B*2*eb* [18]. However, using a model of *B*2*eb* symmetry in combined refinements using both room temperature and 2 K data sets did not give any significant improvement in agreement between the observed and calculated data (for the room temperature data, an R_{wp} of 3.09% was obtained for the disordered model of *I*4/*mmm* symmetry described here, in contrast to an R_{wp} of 3.49% for a model of *B*2*eb* symmetry with an additional 15 variables) and no additional reflections precluded by *I*4/*mmm* symmetry were observed. This suggests that at both 298 and 2 K, the crystal structure is best described by the disordered *I*4/*mmm* structure. Details from the refinement using room temperature data are given in Table 1 with selected bond lengths in Table 2. The refinement profiles and an illustration of the model obtained from the room temperature refinement are given in Figs. 1 and 2, respectively.

3.3. Structure of $Bi_2Sr_2Nb_{2.5}Fe_{0.5}O_{12}$

The structural model obtained in this work is consistent with that suggested by Mandal et al. [11] with significant *B* site ordering, some *M*/*A* site disorder, stoichiometric with respect to oxygen content and with the long-range crystal structure best described using a tetragonal model of *I*4/*mmm* symmetry.

The distribution of Sr^{2+} and Bi^{3+} was refined using combined XRPD and NPD refinements, with constraints applied to maintain overall stoichiometry and ensure that both *A* and *M* sites remained fully occupied. The model obtained from the room temperature data shows that the *A* site is ~18% occupied by Bi^{3+}, and the *M* site ~18% occupied by Sr^{2+} (see Table 1); this level of 18.1(1)% antisite defects over the *M* and *A* sites is consistent with structural work reported elsewhere for related Aurivillius materials [14,15,17]. A likely driving force for this cation disorder is the relief of strain due to size mismatch between the fluorite-like and perovskite blocks. Armstrong et al. [13] calculated the ideal *a* parameter of the $[Bi_2O_2]^{2+}$ blocks to be 3.80 Å and derived an expression for the ideal *a* parameter of the perovskite $[A_2B_3O_{10}]$ blocks:

$$a = 1.33r_R + 0.60r_M + 2.36\,\text{Å}$$

where r_R is the six-coordinate ionic radius of the *B* site cations and r_M the eight-coordinate ionic radius of the *A* site cations. Using mean ionic radii (calculated from radii published by Shannon [19]), the ideal *a* parameter of fully ordered $Bi_2Sr_2Nb_{2.5}Fe_{0.5}O_{12}$ would be 4.07 Å. This is significantly larger than that of the fluorite blocks and the observed *a* parameter of 3.91129(4) Å reflects the compromise reached as a result of reducing this size mismatch.

However, cation disorder is not the only mechanism for relieving this strain in Aurivillius materials. Octahedral tilting within the perovskite blocks can relieve strain by reducing the width of the perovskite blocks and this distortion is observed in the polar Aurivillius materials $Bi_5Ti_3FeO_{15}$ [4,5] and $Bi_4Ti_3O_{12}$ [16]. Octahedral tilting will give rise to displacements, either static or dynamic, of the oxygen sites within the perovskite blocks. If these distortions are ordered over a sufficient length scale, the overall symmetry will be lowered and additional reflections will be observed in long-range diffraction experiments. If the distortions are only local, increased displacement of oxygen atoms along specific directions is observed, reflected by high anisotropic thermal parameters for these sites. The models obtained from refinements using both room temperature and 2 K data sets show such anisotropic thermal parameters. Qualitatively, these are similar to those observed in $Bi_2Sr_{1.4}La_{0.6}Nb_2MnO_{12}$, [6] although those in $Bi_2Sr_2Nb_{2.5}Fe_{0.5}O_{12}$ are much more pronounced. The model for $Bi_2Sr_2Nb_{2.5}Fe_{0.5}O_{12}$ was significantly improved by disordering the equatorial oxygen in the central perovskite layer (O(1)); it was noticeably displaced from its ideal, high symmetry site and the displacement increased slightly on cooling (0.360(1) Å at room temperature, 0.366(1) Å at 2 K). Such disordering in $Bi_2Sr_{1.4}La_{0.6}Nb_2MnO_{12}$ did not improve the model significantly, suggesting that any distortions in this manganese-containing phase are much smaller. The atoms in Fig. 2b are represented by their thermal ellipsoids and it can be observed that the anisotropy is consistent with rotation of the octahedra around both the short axis (suggested by high U_{11} and U_{22} parameters for the apical oxygen sites and high U_{33} parameters for the equatorial oxygen sites) and the long axis (high U_{22} parameters for the equatorial

Table 2
Selected bond lengths determined from combined refinement using room temperature TOF NPD data and room temperature XRPD data for $Bi_2Sr_2Nb_{2.5}Fe_{0.5}O_{12}$

Bi/Sr(*A*)–O(1) × 4	2.635(1)	Fe/Nb(1)–O(1) × 8	1.9885(2)
Bi/Sr(*A*)–O(1) × 4	3.124(1)		
Bi/Sr(*A*)–O(3) × 4	2.76841(7)	Fe/Nb(1)–O(3) × 2	1.975(1)
Bi/Sr(*A*)–O(5) × 4	2.6818(8)	Fe/Nb(2)–O(3) × 1	2.257(1)
Bi/Sr(*M*)–O(2) × 4	2.3045(5)	Fe/Nb(2)–O(4) × 1	1.813(1)
Bi/Sr(*M*)–O(4) × 4	2.9613(6)	Fe/Nb(2)–O(5) × 4	1.9784(2)

Table 1
Details from combined refinement using room temperature TOF NPD data and room temperature XRPD data for $Bi_2Sr_2Nb_{2.5}Fe_{0.5}O_{12}$

Atom	*z*	Frac.	U_{11} × 100 (Å^2)	U_{22} × 100 (Å^2)	U_{33} × 100 (Å^2)
Bi/Sr(*A*)	0.06301(3)	0.181(2)/0.819(2)	1.12(1)	1.12(1)	1.80(5)
Bi/Sr(*M*)	0.21338(8)	0.819(2)/0.181(3)	2.21(2)	2.21(2)	2.55(5)
Fe/Nb(1)	0.5	0.353(7)/0.647(7)	0.13(2)	0.13(2)	0.52(5)
Fe/Nb(2)	0.37288(2)	0.073(3)/0.927(3)	0.46(1)	0.46(1)	0.56(4)
O(1)	0.0	0.5[a]	0.21(3)	0.34(4)	1.68(7)
O(2)	0.25	1[a]	0.89(3)	0.89(3)	0.47(1)
O(3)	0.44068(3)	1[a]	2.22(3)	2.22(3)	0.24(5)
O(4)	0.31842(3)	1[a]	4.16(6)	4.16(6)	0.40(6)
O(5)	0.11814(2)	1[a]	0.39(2)	0.97(3)	2.48(5)

Refinements were carried out in space group *I*4/*mmm* with *A*, *M* and *B*(2) cations and O(3) and O(4) on the 4*e* site (0,0,*z*), *B*(1) cations on 2*b* site (0,0,$\frac{1}{2}$), O(1) on the 8*i* site (0,*x*,0) where $x = 0.4080(3)$, O(2) on the 4*d* site and O(5) on the 8*g* site (0,$\frac{1}{2}$,*z*).
$a = 3.91129(4)$, $c = 33.2876(4)$ Å.
$\chi^2 = 4.736$, $R_{wp} = 3.09\%$, $R_p = 3.15\%$.
[a] Fractional occupancy fixed, see text.

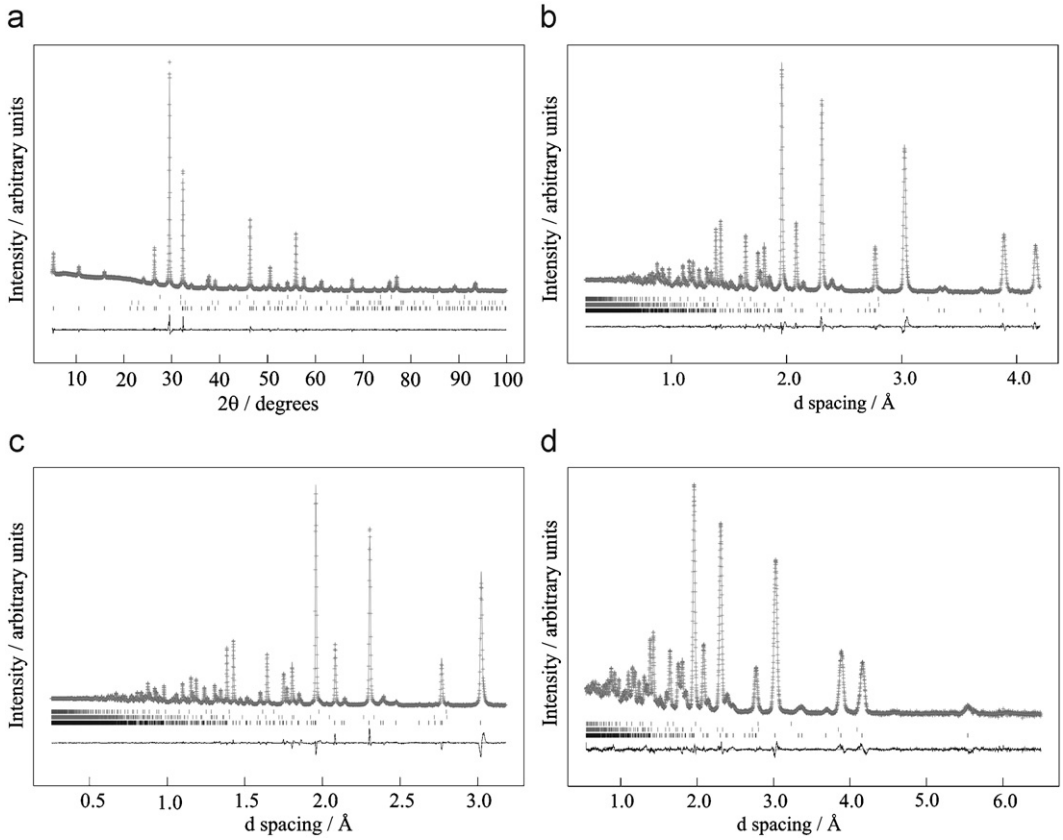

Fig. 1.

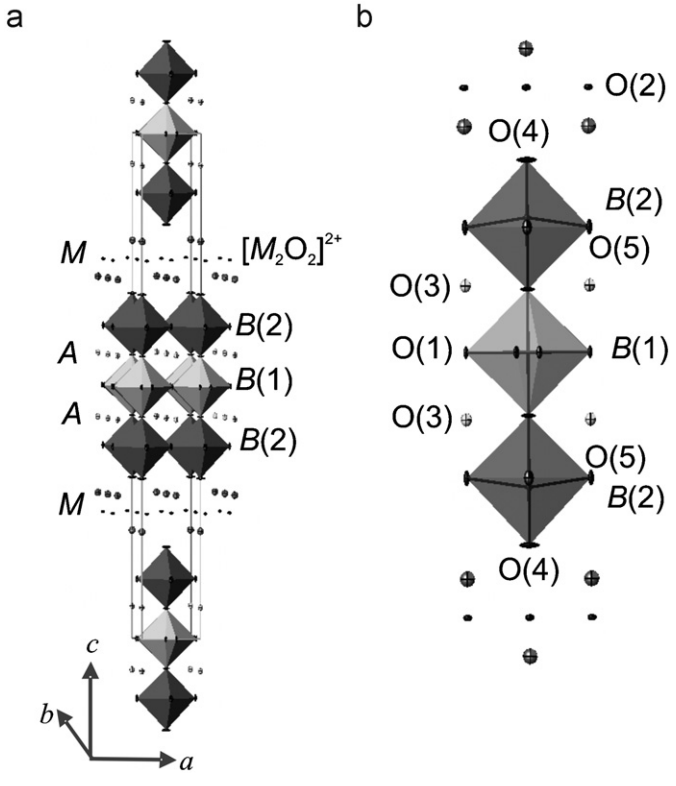

Fig. 2.

oxygen sites). The distortion is much more pronounced for the central layer of the perovskite blocks. These results suggest that although the long-range structure of this material is best described by a high symmetry, *I*4/*mmm* model, the local structure may in fact be distorted with some rotation of octahedra around both the long and short axes. This insight into the likely distorted local structure of the material can be gained due to the increased sensitivity of NPD data to scattering due to the lighter oxygen sights compared with XRPD data. Future work to probe this possible distortion should involve techniques more sensitive to local structure such as X-ray absorption spectroscopy.

As noted by Sharma et al. [10] given that this research was driven by the search for multiferroic materials, the observation that the long-range crystal structures of $Bi_2Sr_2Nb_{2.5}Fe_{0.5}O_{12}$ and of a number of similar Aurivillius materials are described by centrosymmetric *I*4/*mmm* symmetry, rather than a polar symmetry, is interesting. However, this can be rationalised by considering the degree of size mismatch present in these materials. As discussed, an ordered model of $Bi_2Sr_2Nb_{2.5}Fe_{0.5}O_{12}$ would exhibit significant size mismatch but this is relieved by cation disorder between the larger Sr^{2+} and smaller Bi^{3+} cations over the *M* and *A* sites. In $Bi_{1.5}Sr_{2.5}Nb_{2.5}Ru_{0.5}O_{12}$, the presence of larger *B* site cations than in the orthorhombic $Bi_2Sr_2Nb_2TiO_{12}$ yet the surprising absence of octahedral tilting [10] may again be rationalised in terms of reduced size mismatch. The majority of the additional Sr^{2+} cations are located in the fluorite *M* site [10], increasing the width of this layer and so reducing the stacking strain and the tendency for octahedral tilting.

The tilting of the octahedra will reduce strain and relieve overbonding of the *B* site cations and the larger distortion of the

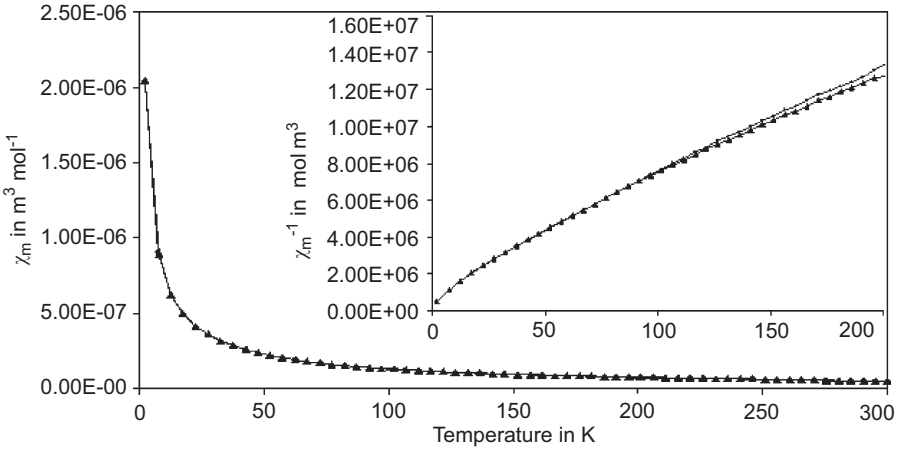

Fig. 3.

central layer may be due to the mixed occupancy of Fe^{3+} and Nb^{5+} cations, compared with the outer layers occupied almost entirely by Nb^{5+}. Bond valence sum (BVS) calculations [20] suggest that in the central layer, the Fe^{3+} cation is overbonded (calculated valence of +3.268) while the Nb^{5+} cation is very slightly underbonded (calculated valence of +4.928). In the outer site, the niobium is again almost ideally bonded (calculated valence of +5.030) whereas the iron is more overbonded (calculated valence of +3.335). These calculations suggest that the distortions can be attributed more to the Fe^{3+} cation, requiring a larger coordination polyhedron than Nb^{5+}; this would be consistent with the more pronounced distortion of the central iron-containing layer. However, it must be noted that for such mixed occupancy of a given site, average bond distances inherently restrict the reliability of such BVS estimates.

A high level of cation ordering over the *B* sites is observed, with most of the iron located in the central, high symmetry *B*(1) site. As suggested by Mandal et al. [11], the driving force for this ordering could be the out-of-centre displacement taking place in the lower symmetry *B*(2) sites. The extent of this out-of-centre displacement is illustrated by the significant difference in apical bond lengths between *B*(2) and the apical oxygens O(3) and O(4), with the longer bond (2.257(1) Å) to O(3) within the perovskite blocks, and the much shorter *B*(2)–O(4) bond (1.813(1) Å) towards the fluorite-like layers. The displacement observed in $Bi_2Sr_2Nb_{2.5}Fe_{0.5}O_{12}$ is slightly larger than that observed in $Bi_2Sr_{1.4}La_{0.6}Nb_2MnO_{12}$.

For a high spin, octahedrally coordinated d^5 cation, an out-of-centre displacement would not result in any loss of crystal field stabilisation energy, so if the displacement is simply electrostatic in origin, this would not provide a driving force for this ordering. However, if the origin of this displacement is the second-order Jahn–Teller effect (SOJT), this would favour a *B* site ordered model as d^n cations cannot undergo SOJT distortions. It is interesting that such a high level of *B* site ordering is observed in $Bi_2Sr_2Nb_{2.5}Fe_{0.5}O_{12}$, while a very careful structural investigation of $Bi_5Ti_3FeO_{15}$ revealed a statistical distribution of iron and titanium over the two *B* sites. Incidentally, no significant out-of-centre displacement was observed in this $n = 4$ material. It is possible that the *B* site cation ordering is electrostatically driven, during formation of the structure. On electrostatic grounds, it would be favourable for the more highly charged *B* site cation to be located in the outer perovskite layers, closer to the fluorite layers containing the central layer of oxygen anions, rather than in the central layer with *B* site cations above and below. The effect would become more pronounced in *M*–*A* cation disordered systems where the *A* cation is divalent. Once in the outer, lower symmetry *B* site, the cation can undergo an out-of-centre displacement, driven either by electrostatic effects or by the SOJT. The lack of *B* site ordering in $Bi_5Ti_3FeO_{15}$ may be a result of the similar size and charge of Fe^{3+} and Ti^{4+}; there would be less electrostatic drive for them to order during synthesis.

3.4. Magnetic characterisation of $Bi_2Sr_2Nb_{2.5}Fe_{0.5}O_{12}$

A plot of susceptibility versus temperature is given in Fig. 3; the inset shows the variation of inverse susceptibility with temperature. The material displays almost ideal Curie–Weiss paramagnetism in the temperature range studied, with a Weiss constant of −16.1 K (from FC data) and a paramagnetic moment of 3.20 μ_B per formula unit. This moment is lower than the expected value for half a mole of Fe^{3+} per formula unit (expected value of 4.19 μ_B). Exchange interactions between d^5 Fe^{3+} cations would be expected to give antiferromagnetic interactions which could account for the low moment. This is consistent with the negative Weiss constant observed, reflecting the presence of some local interactions of an antiferromagnetic nature. It is noted that a lower than expected paramagnetic moment for Fe^{3+} in the structurally related material $LaSr_3FeGa_2O_9$ is ascribed to the presence some intermediate spin Fe^{3+} cations [21].

4. Conclusions

In conclusion, we report here the synthesis as well as the structural and magnetic characterisation of the $n = 3$ Aurivillius material $Bi_2Sr_2Nb_{2.5}Fe_{0.5}O_{12}$. Rietveld refinements using both NPD and XRPD data reveal structural features in agreement with previous work, including significant ordering of Fe^{3+} and Nb^{5+} cations over the two *B* sites and some disorder of Sr^{2+} and Bi^{3+} cations over the *M* and *A* sites. However, due to the increased sensitivity of NPD data to scattering from lighter atoms compared with XRPD data, further information on the oxygen sites has been obtained. These results confirm that the material is stoichiometric with respect to oxygen and provide evidence for some short range distortion of the perovskite blocks, consisting of local rotation of octahedra. Magnetic measurements indicate that the material behaves as a Curie–Weiss paramagnet in the temperature range studied, with no evidence of long-range magnetic interactions. This is perhaps unsurprising given the disordered and mixed occupancy of the central perovskite layer by Fe^{3+} and Nb^{5+} cations.

Acknowledgments

We thank EPSRC for financial support and ISIS for the provision of neutron diffraction facilities. We are very grateful to Dr. R. Smith for experimental assistance with the collection of NPD data and to Prof. F.J. Berry for very useful discussions.

References

[1] B. Aurivillius, Ark. Kemi. 1 (1949) 499.
[2] C.A-P. de Araujo, J.D. Cuchiaro, L.D. McMillan, M.C. Scott, J.F. Scott, Nature 374 (1995) 627.
[3] K.A. Yee, T.A. Albright, D. Jung, M.-H. Whangbo, Angew. Chem. Int. Ed. Engl. 28 (6) (1989) 750.
[4] C.H. Hervoches, A. Snedden, R. Riggs, S.H. Kilcoyne, P. Manuel, P. Lightfoot, J. Solid State Chem. 164 (2002) 280.
[5] A. Snedden, C.H. Hervoches, P. Lightfoot, Phys. Rev. B 67 (2003) 092102.
[6] E.E. McCabe, C. Greaves, J. Mater. Chem. 15 (2005) 177.
[7] W.J. Yu, Y.I. Kim, D.H. Ha, J.H. Lee, Y.K. Park, S. Seong, N.H. Hur, Solid State Commun. 11 (1999) 705.
[8] E.I. Henriques, H.J. Kim, M.S. Haluska, D.D. Edwards, S.T. Misture, Solid State Ionics 178 (2007) 1175–1179.
[9] M. Tripathy, R. Mani, J. Gopalakrishnan, Mater. Res. Bull. 42 (2007) 950–960.
[10] N. Sharma, C.D. Ling, G.E. Wrighter, P.Y. Chen, B.J. Kennedy, P.L. Lee, J. Solid State Chem. 180 (2007) 370–376.
[11] T.K. Mandal, T. Sivakumar, S. Augustine, J. Gopalakrishnan, Mater. Sci. Eng. B 121 (2005) 112.
[12] A.C. Larson, R.B. von Dreele, Los Alamos National Laboratory Report: LA-UR-86-748, 1987.
[13] R.A. Armstrong, R.E. Newnham, Mater. Res. Bull. 7 (1972) 1025.
[14] S.M. Blake, M.J. Falconer, M.M. McCreedy, P. Lightfoot, J. Mater. Chem. 7 (8) (1997) 1609.
[15] M.S. Haluska, S.T. Misture, J. Solid State Chem. 177 (2004) 1965.
[16] C.H. Hervoches, P. Lightfoot, J. Solid State Chem. 153 (2000) 66.
[17] N.C. Hyatt, J.A. Hriljac, T.P. Comyn, Mater. Res. Bull. 38 (2003) 837.
[18] R.E. Newnham, R.W. Wolfe, J.F. Dorrian, Mater. Res. Bull. 6 (1971) 1029.
[19] R.D. Shannon, Acta Crystallogr. A 32 (1976) 751.
[20] I.D. Brown, D. Altermatt, Acta Crystallogr. B 41 (1985) 244.
[21] B. Shankar, H. Steinfink, J. Solid State Chem. 122 (1996) 390–393.